

Anomalous properties of hexagonal rare-earth ferrites from first principlesChangsong Xu,^{1,2} Yurong Yang,² Shanying Wang,¹ Wenhui Duan,¹ Binglin Gu,³ and L. Bellaiche²¹*State Key Laboratory of Low-Dimensional Quantum Physics and Collaborative Innovation Center of Quantum Matter, Department of Physics, Tsinghua University, Beijing 100084, China*²*Physics Department and Institute for Nanoscience and Engineering, University of Arkansas, Fayetteville, Arkansas 72701, USA*³*Institute for Advanced Study, Tsinghua University, Beijing 100084, China*

(Received 17 January 2014; published 22 May 2014)

First-principles calculations are performed to predict structural, electric, magnetic, and magnetoelectric properties of hexagonal rare-earth ferrites ($R\text{FeO}_3$) under chemical and hydrostatic pressures. Decreasing the rare-earth ionic radius has two dramatic consequences: (i) an enhancement of the electrical polarization by a factor of 60% and (ii) a magnetic transition, which renders the systems (weakly) ferromagnetic. Moreover and unlike conventional ferroelectrics, the electrical polarization strengthens as a hydrostatic pressure is applied and increases in magnitude in any hexagonal rare-earth ferrites. Finally, applying a hydrostatic pressure in $R\text{FeO}_3$ having small or intermediate rare-earth ionic radius results in the sudden disappearance of a weak magnetization and of the linear magnetoelectric effect above some critical pressure. Origins of these striking effects are revealed.

DOI: [10.1103/PhysRevB.89.205122](https://doi.org/10.1103/PhysRevB.89.205122)

PACS number(s): 75.85.+t, 61.50.Ah, 61.50.Ks, 75.30.-m

I. INTRODUCTION

Multiferroics exhibit a coexistence of an electrical polarization and magnetic ordering, with these two quantities being coupled via the magnetoelectric effect [1,2]. As such, it has now long been expected that they will lead to a breakthrough in spintronics and memory devices [3]. An important requirement for these realizations is that the material must be multiferroic at room temperature, which explains the flurry of activities on BiFeO_3 [4,5]. However, another material has been recently found to be multiferroic at room temperature, that is hexagonal LuFeO_3 [6–8]. Such compound was also recently predicted to possess a weak magnetization and a *linear* magnetoelectric effect (as a result of an original coupling), which further emphasize its importance and interest [9].

Hexagonal LuFeO_3 is a member of the broad family formed by the hexagonal rare-earth ferrites, $R\text{FeO}_3$, where R is a rare-earth ion. Surprisingly and unlike orthoferrites (see, Ref. [10] and references therein), only materials made of small rare-earth ions (e.g., $R = \text{Ho}, \text{Er}, \text{Tm}, \text{Yb}, \text{Lu}$) have been investigated so far in this family. It is thus presently unknown how their structural, electric, magnetic, and magnetoelectric properties depend on chemical pressure, that is, on the size of the rare-earth ion. For instance, is it possible that hexagonal rare-earth ferrites with larger R (e.g., $\text{Ce}, \text{Pr}, \text{or Nd}$) exhibit an electrical polarization that is very different in magnitude than that of LuFeO_3 ? Similarly, can the magnetic ground state be sensitive to the size of the R element? In other words, can chemical pressure tailor the magnitude of the electrical polarization and induce a magnetic phase transition? Such questions, which are also relevant to magnetoelectricity, have not been addressed despite their obvious fundamental and technological importance.

Another kind of pressure that can affect material properties is the hydrostatic pressure [10–12]. However, we are not aware that any study devoted to the investigation of the effect of hydrostatic pressure on hexagonal rare-earth ferrites has ever been attempted. This is unfortunate since, e.g., hexagonal $R\text{FeO}_3$ (as well as hexagonal rare-earth manganites [13,14]) are improper ferroelectrics and thus have the potential to

display pressure-induced properties that are not present in conventional ferroelectrics.

Here, we use first principles to reveal how structural, electric, magnetic, and magnetoelectric properties of hexagonal rare-earth ferrites depend on chemical and hydrostatic pressures. As we will see, surprises are in store. Examples are a large relative enhancement (about 60%) of the electrical polarization and the occurrence of a magnetic transition, when studying hexagonal $R\text{FeO}_3$ with small versus large ionic rare-earth radius. Other examples include the anomalous increase of the electrical polarization with hydrostatic pressure in any hexagonal rare-earth ferrite, and the possibility of turning on and off linear magnetoelectric effect and weak magnetization.

The paper is organized as follows. Section II provides details about the computational methods used here. In Sec. III, we present and discuss the results. Finally, the present work is summarized in Sec. IV.

II. COMPUTATIONAL METHODS

Density-functional calculations are performed using the Vienna *ab initio* simulation package (VASP) [15] to investigate hexagonal $R\text{FeO}_3$, with $R = \text{Ce}, \text{Pr}, \text{Nd}, \text{Pm}, \text{Sm}, \text{Gd}, \text{Tb}, \text{Dy}, \text{Ho}, \text{Er}, \text{Tm}, \text{and Lu}$. Technically, the generalized gradient approximation (GGA), together with the PBE functional for solids [16], is used since it is known to provide accurate structural parameters [17]. We employ the projected augmented wave (PAW) method to mimic electron-ion interactions and the localized Fe $3d$ electrons are treated with an effective Hubbard $U = 4$ eV [17]. A 30-atom cell is simulated to mimic the polar $P6_3\text{cm}$ phase [see Figs. 1(a) and 1(b)]. We study four possible noncollinear magnetic structures that have been suggested in hexagonal LuFeO_3 [8] and that are the $\Gamma_1, \Gamma_2, \Gamma_3,$ and Γ_4 states [21]. They are schematized in Figs. 1(c)–1(f). Eleven valence electrons ($5s^25p^65d^16s^2$) are considered for Ce, Pr, Nd, Pm, and Sm, while nine valence electrons ($5p^65d^16s^2$) are taken for Gd, Tb, Dy, Ho, Er, Tm, and Lu. The number of valence electrons chosen for Fe and O are 8 ($3d^64s^2$) and 6 ($2s^22p^4$), respectively. As in Ref. [9],

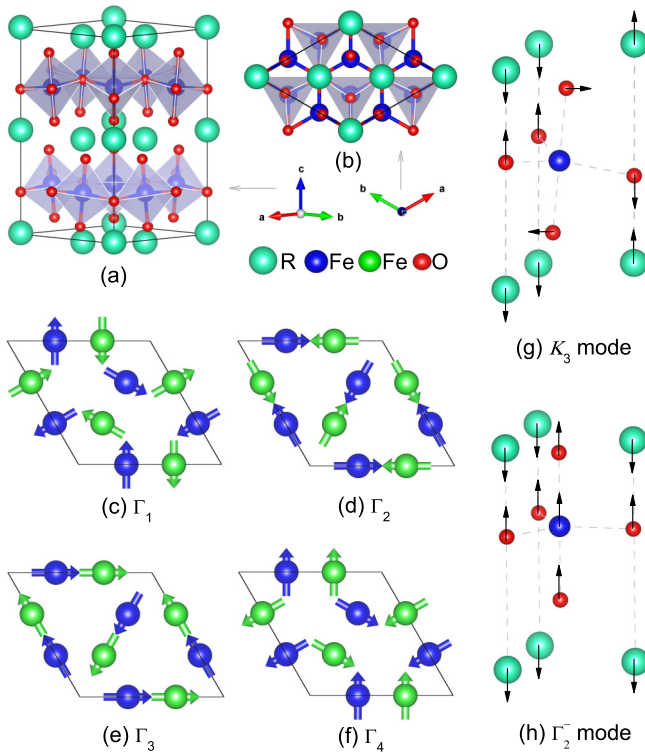


FIG. 1. (Color online) Schematics of structure, magnetic arrangements, and phonon modes in hexagonal $R\text{FeO}_3$. (a) and (b) show the side and top views of the $P6_3cm$ structure, respectively. (c), (d), (e), and (f) show the magnetic arrangements Γ_1 , Γ_2 , Γ_3 , and Γ_4 , respectively. In (c)–(f), the Fe ions of the top layer are displayed in bright green while those in the layer below are shown in blue. (g) and (h) show the atomic pattern associated with the K_3 and Γ_2^- phonon modes, respectively.

we keep the $4f$ electrons of the R ions in the core, because (i) convergence of results is typically difficult to achieve if these $4f$ electrons are incorporated in the valence; (ii) we are not presently interested in the subtle properties originating from the possible occurrence of magnetism associated with rare-earth elements at low temperature (see, e.g., Ref. [18] and references therein). For instance, Ref. [18] showed that Nd ions in NdFeO_3 orthoferrite begin to magnetically order at around 100 K (which is one of the highest magnetic ordering temperature for rare-earth ions in orthoferrites). Moreover, there is no magnetic ordering associated with rare-earth ions in LuFeO_3 because the $4f$ shells are filled. The results about magnetism indicated in this paper for all investigated hexagonal $R\text{FeO}_3$ materials should thus be valid above critical temperatures that are rather low (i.e., of the order of 100 K or even smaller in some cases); and (iii) we numerically checked that the inclusion of the $4f$ electrons of the R ions in the valence has a rather small effect on structural properties of hexagonal $R\text{FeO}_3$ system. For instance, such inclusion only modifies the a lattice parameter, the c lattice constant and the electrical polarization of hexagonal GdFeO_3 by 0.15%, 0.38%, and 2.63%, respectively, with respect to the case when these $4f$ electrons are frozen in the core. We also further found that the in-plane (J_1) and out-of-plane (J_2) magnetic exchange parameters between Fe ions are rather

insensitive to this inclusion, as demonstrated by the fact that J_1 (respectively, J_2) of hexagonal GdFeO_3 only varies from 33.9 to 33.2 meV (respectively, from 0.9 to 1.5 meV), when moving these $4f$ electrons from the core to the valence. Furthermore, spin-orbit coupling and noncollinear magnetism are included in all simulations. Technically, a 500 eV plane wave energy cutoff [14] is used and the atomic configuration is assumed to be converged when the Hellman-Feynman forces are equal to, or smaller than, 0.001 eV/Å. A $4 \times 4 \times 2$ Γ -centered k -point mesh is first used to obtain the structure and magnetic arrangement. A denser $6 \times 6 \times 3$ k -point mesh is then employed to refine magnetic properties and energies (these latter being converged within 10^{-8} eV). The polarization is calculated using the modern (Berry-phase) theory of polarization [19], and the phonon modes are identified (and their amplitudes computed) by the AMPLIMODES software [20].

For the computations related to hydrostatic pressure, we first take advantage of the PSTRESS option of VASP [15]. The calculations are then refined by determining the lattice vectors and atomic displacements that minimize the internal energy for different fixed volumes. The second-order Birch-Murnaghan equation of state:

$$E(V) = E_0 + \frac{9}{8} B_0 V_0 \left[\left(\frac{V_0}{V} \right)^{\frac{2}{3}} - 1 \right]^2 \quad (1)$$

is then used to fit the energy-versus-volume function, where B_0 is the bulk modulus and V_0 is the equilibrium volume. Pressure (which is computed as $P = -\frac{dE}{dV}$) and enthalpy (which is equal to $E + PV$) are finally extracted from this equation of state and its fitted parameters.

III. RESULTS

Figures 2(a) and 2(b) show the evolution of the a and c lattice parameters, and the resulting c/a ratio and volume V , of the $P6_3cm$ state, as a function of the ionic radius (r_R) of the rare-earth element [22], respectively. The lattice parameters and volume all decrease when r_R decreases, as consistent with the concept of chemical pressure inherent to the decrease of the rare-earth ionic radius. For instance, a , c , and V are reduced by 7.7%, 1.9%, and 16.3%, respectively, when going from CeFeO_3 to LuFeO_3 . On the other hand, chemical pressure enhances the c/a ratio by 6.3% during these variations. Note that the predicted lattice constants of LuFeO_3 are $a = 5.915$ Å and $c = 11.572$ Å, which agree rather well (namely, around 1%) with the experimental data of Ref. [7] yielding $a = 5.965$ Å and $c = 11.702$ Å. The resulting predicted and measured axial ratio are therefore both close to 1.96 and agree with each other within 0.3%. Similarly, our predicted axial ratio for ErFeO_3 and TmFeO_3 bulks agree within 1.1% and 0.08% with those reported in Ref. [6] for ErFeO_3 and TmFeO_3 films, respectively. Such comparisons attest to the accuracy of our simulations.

Moreover, Fig. 2(c) indicates that the electronic polarization (which is oriented along the c axis) increases in magnitude when r_R decreases. This behavior is qualitatively consistent with the results of Ref. [9]. However, the investigated rare-earth elements in this latter work [9] were only Ho, Er, Tm, Yb, Lu, which are among the smallest ones. As a result, Fig. 2(c) indicates that the polarization (P) only changes by $\simeq 6\%$ within

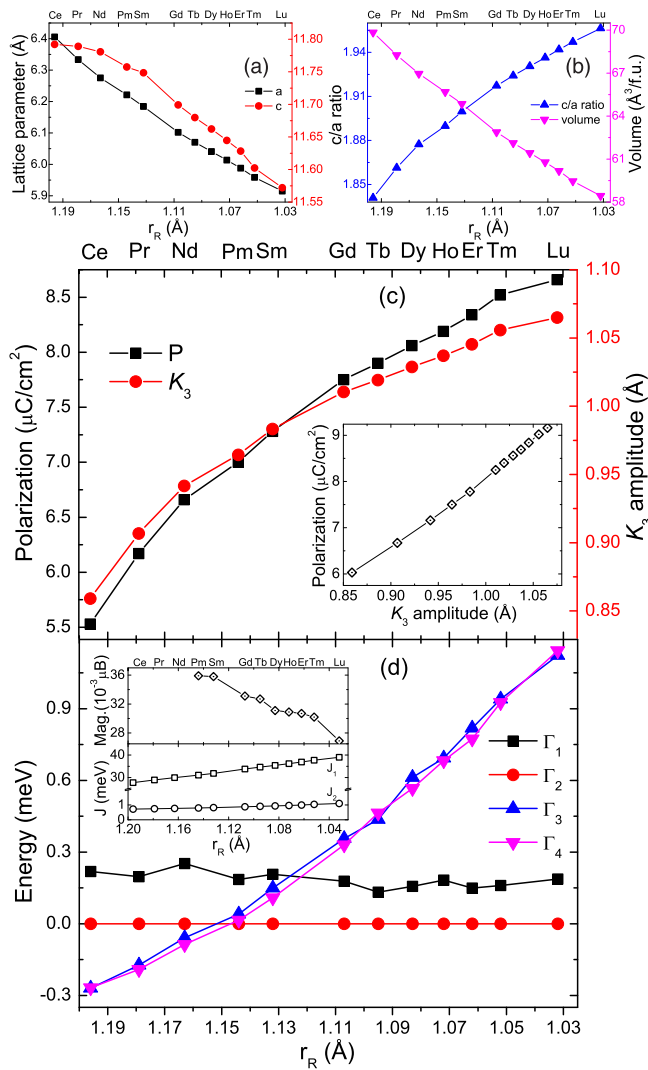


FIG. 2. (Color online) Predicted properties of hexagonal $R\text{FeO}_3$ as a function of the rare-earth ionic radius. (a) shows the lattice constants a and c . (b) displays the c/a axial ratio and the volume per formula unit. (c) reports the magnitude of the polarization and amplitude of the K_3 mode, with its inset revealing the relationship between these two quantities. (d) shows the total energies of the Γ_1 , Γ_2 , Γ_3 , and Γ_4 noncollinear magnetic arrangements, with the zero of energy corresponding to Γ_2 . The top inset of (d) displays the weak magnetization inherent to Γ_2 . The bottom inset shows the in-plane (J_1) and out-of-plane (J_2) magnetic exchange coefficients between Fe ions [36].

this set of elements (which is comparable with the variation of 9% found in Ref. [9]). In contrast, Fig. 2(c) shows that the change in polarization is much larger (around 60%) when considering the variation from CeFeO_3 ($P = 5.5 \mu\text{C}/\text{cm}^2$) to LuFeO_3 ($P = 8.7 \mu\text{C}/\text{cm}^2$). Let us try to understand the mechanism responsible for such large enhancement. For that, it is important to recall that previous studies [9,14] revealed that hexagonal $R\text{FeO}_3$ are improper ferroelectrics. In other words, the polarization (associated with the so-called Γ_2^- mode) is only a secondary mode and the right order parameter responsible for the transformation from paraelectric $P6_3/mmc$ to polar $P6_3cm$ is another mode, namely K_3

[see Figs. 1(g) and 1(h)]. This K_3 mode is associated with the tilt of FeO_5 bipyramid and the buckling of the R -O plane. Figure 2(c) shows that chemical pressure considerably strengthens the magnitude of the K_3 mode, and, as a result of the collaborative coupling between K_3 and polarization, leads to an enhancement of the polarization. Such collaboration is further demonstrated in the inset of Fig. 2(c), which reports the almost perfect linear relationship between the polarization and amplitude of the K_3 mode.

Furthermore, Fig. 2(d) reveals an important and previously unknown feature of magnetism in hexagonal $R\text{FeO}_3$: the three largest rare-earth elements (Ce, Pr, and Nd) have Γ_4 for their magnetic ground state (with Γ_3 being extremely close in energy) while the other R ions possess a Γ_2 magnetic ground state—with Γ_1 being about 0.2 meV-per-30 atoms higher in energy (the fact that our simulations indicate that Γ_2 is the most stable magnetic state of hexagonal LuFeO_3 is consistent with previous works [8,9]). In other words, chemical pressure induces a magnetic phase transition from Γ_4 to Γ_2 for a rare-earth ionic radius that is very close to the one of Pm [23]. Such magnetic transition renders the hexagonal ferrites having smaller r_R both ferroelectric and ferromagnetic because Γ_2 exhibits a (weak) magnetization along the c axis, unlike Γ_4 [21]. The dependency of this weak magnetization, M , on the rare-earth ionic radius is displayed in the top inset of Fig. 2(d), which reveals a slight decrease of M with r_R . Figures 2(c) and 2(d) therefore imply that the (P, M) combination can be adjusted by playing with chemical pressure in the nine smallest rare-earth elements considered here. Furthermore, the bottom inset of Fig. 2(d) shows the evolution of the in-plane (J_1) and the out-of-plane (J_2) magnetic exchange coefficients between Fe ions predicted by our first-principles calculations as a function of r_R . Note that the J_1 and J_2 parameters are such that the corresponding Heisenberg model is given by $H = \frac{1}{2} J_1 \sum_{i,j} \mathbf{S}_i \cdot \mathbf{S}_j + \frac{1}{2} J_2 \sum_{i,j} \mathbf{S}_i \cdot \mathbf{S}_j$. Here, the magnitude of the spins \mathbf{S}_i and \mathbf{S}_j are the unity, and the sums over i run over all the Fe sites, while the first (second) sum over j runs over Fe ions that are nearest neighbors, along in-plane (out-of-plane) directions, of the Fe ions that are located at the site i . One can see that (i) both J_1 and J_2 are positive, which is indicative of a predominant antiferromagnetic order below a critical temperature (as consistent with the Γ_1 , Γ_2 , Γ_3 , and Γ_4 structures studied here); (ii) J_2 is negligible with respect to J_1 for any hexagonal $R\text{FeO}_3$ bulk (J_2 is typically 40 times smaller than J_1); and J_1 significantly decreases as r_R increases (e.g., it decreases by around 30% when going from Lu to Ce), which naturally implies that the (highest) critical temperature at which a long-range magnetic ordering forms is highly adjustable by chemical pressure. Interestingly, the decrease of J_1 from 39.0 to 27.7 meV when going from Lu to Ce leads to the prediction that hexagonal CeFeO_3 should order magnetically very close to room temperature (i.e., at around 313 K) if one recalls that the experimental Neel temperature of LuFeO_3 is 440 K [8] and assumes that these Neel temperatures are directly proportional to J_1 . As a result, large magnetoelectricity should occur in CeFeO_3 at room temperature.

Let us now choose three materials and predict the effect of hydrostatic pressure on their properties [24]. They are hexagonal CeFeO_3 (large r_R), GdFeO_3 (intermediate r_R) and LuFeO_3 (small r_R). As shown by Fig. 2(d), the magnetic

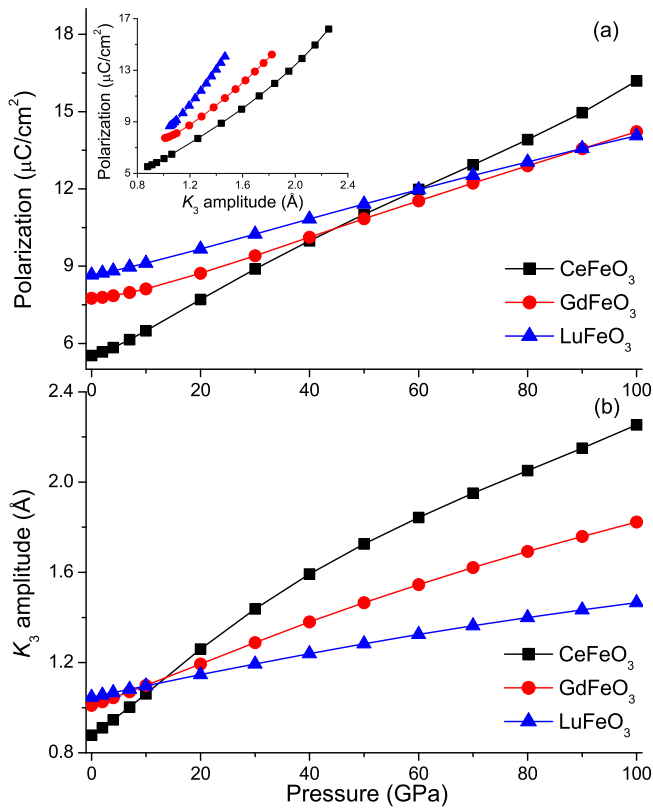


FIG. 3. (Color online) Polarization (a) and K_3 amplitude (b) of CeFeO_3 , GdFeO_3 , and LuFeO_3 , as a function of hydrostatic pressure. The inset of (a) reports the polarization versus the amplitude of the K_3 mode.

ground state of hexagonal CeFeO_3 is Γ_4 , while it is Γ_2 for both hexagonal GdFeO_3 and LuFeO_3 compounds.

One particularly striking feature revealed by Fig. 3(a) is that the electrical polarization of any of these three compounds (and thus of any hexagonal $R\text{FeO}_3$) is enhanced when the hydrostatic pressure is increased. Such behavior is contradictory to the common knowledge that P should decrease and even vanish when increasing hydrostatic pressure [11] as a result of the facts that (i) polarization results from a competition between long-range Coulomb interactions (that favors ferroelectricity) and short-range interactions (which favors the paraelectric structure) [25,26], and that (ii) hydrostatic pressure tips this delicate balance in favor of short-range interactions, thus pushing the system towards paraelectricity [11,27]. Note also that an unexpected pressure-induced enhancement of the polarization was recently predicted to occur in PbTiO_3 and other ABO_3 perovskites [12,28–30]. However, such enhancement typically occurs at very high pressure, that is P first decreases in magnitude with pressure for small pressure before increasing with pressure for larger pressure. Such latter nonmonotonic behavior contrasts with the continuous increase of the polarization shown in Fig. 3(a). These facts therefore hint towards a nonconventional mechanism for the pressure behavior of the polarization in hexagonal $R\text{FeO}_3$. Such mechanism resides in the improper character of P . As a matter of fact, Fig. 3(b) clearly shows that the amplitude of the primary order parameter, that is the K_3 mode, increases

with pressure (the behavior of K_3 with hydrostatic pressure is reminiscent of the pressure-induced increase of the oxygen octahedral tiltings in perovskites [31,32]). As a result of the collaborative coupling between the K_3 and Γ_2^- modes, the induced electrical polarization is therefore also enhanced with hydrostatic pressure, for any pressure. This collaborative coupling is further demonstrated in the inset of Fig. 3(a), that shows that P increases with the amplitude of K_3 in any of the three hexagonal ferrites investigated under hydrostatic pressure.

Another previously unknown behavior of hexagonal $R\text{FeO}_3$ concerns the pressure-induced decrease of the enthalpies of Γ_4 and Γ_3 with respect to that of Γ_2 (see Figs. 4(a)–4(c) for CeFeO_3 , GdFeO_3 , and LuFeO_3 , respectively). Such trend is opposite to the destabilization of Γ_4 in favor of Γ_2 occurring under chemical pressure and depicted in Fig. 2(d). As a result of these opposite behaviors (which emphasize again [10,33] that chemical and hydrostatic pressures differently affect properties, unlike commonly believed [34]), GdFeO_3 and LuFeO_3 systems undergo a magnetic phase transition from Γ_2 to Γ_4 , for a critical pressure of around 30 and 20 GPa, respectively [35]. On the other hand, the magnetic ground state of CeFeO_3 remains Γ_4 up to 100 GPa. The magnetic transition exhibited by both hexagonal GdFeO_3 and LuFeO_3 therefore leads to the sudden disappearance of the magnetization, as shown in the top insets of Figs. 4(b) and 4(c). Furthermore, the weak magnetization inherent to Γ_2 increases in both GdFeO_3 and LuFeO_3 , when increasing the hydrostatic pressure up to its critical value. Such result can be understood by realizing that (i) the magnetization of Γ_2 has been recently found [9] to be induced by the K_3 mode in hexagonal $R\text{FeO}_3$, and (ii) Fig. 3(b) shows that hydrostatic pressure does increase the amplitude of K_3 in GdFeO_3 and LuFeO_3 . Moreover, we previously discussed the fact that the electrical polarization also depends on hydrostatic pressure, via the pressure-induced change in the K_3 mode. On the other hand and as shown in the lower inset of Figs. 4(b) and 4(c), the ratio between the magnetization and polarization is nearly insensitive to the hydrostatic pressure in hexagonal GdFeO_3 and LuFeO_3 for small pressure (for which the magnetic Γ_2 structure is stabilized). In other words, these two materials do exhibit a linear magnetoelectric effect (as found in Ref. [9]) but it is more or less independent of the hydrostatic pressure (especially for GdFeO_3). However, when the pressure is strong enough and that hexagonal GdFeO_3 and LuFeO_3 transform into Γ_4 , the magnetization disappears and thus no linear magnetoelectricity can develop. Magnetic properties and magnetoelectricity of hexagonal GdFeO_3 and LuFeO_3 can thus be turned on and off when playing with hydrostatic pressure, as a result of a magnetic phase transition. One should therefore always check that a variation of K_3 and of P is not accompanied by a magnetic transition before investigating subtle effects (such as bulk magnetoelectricity [9]) because (i) these latter effects can only exist in some magnetic structures and not in others, and (ii) magnetic transitions can easily happen by varying physical factors in hexagonal $R\text{FeO}_3$. Moreover, the inset of Fig. 4(a) further reveals a general feature found in any hexagonal $R\text{FeO}_3$ system, namely that their in-plane magnetic exchange coefficient between Fe ions dramatically increases with hydrostatic pressure. For instance, it more than triples

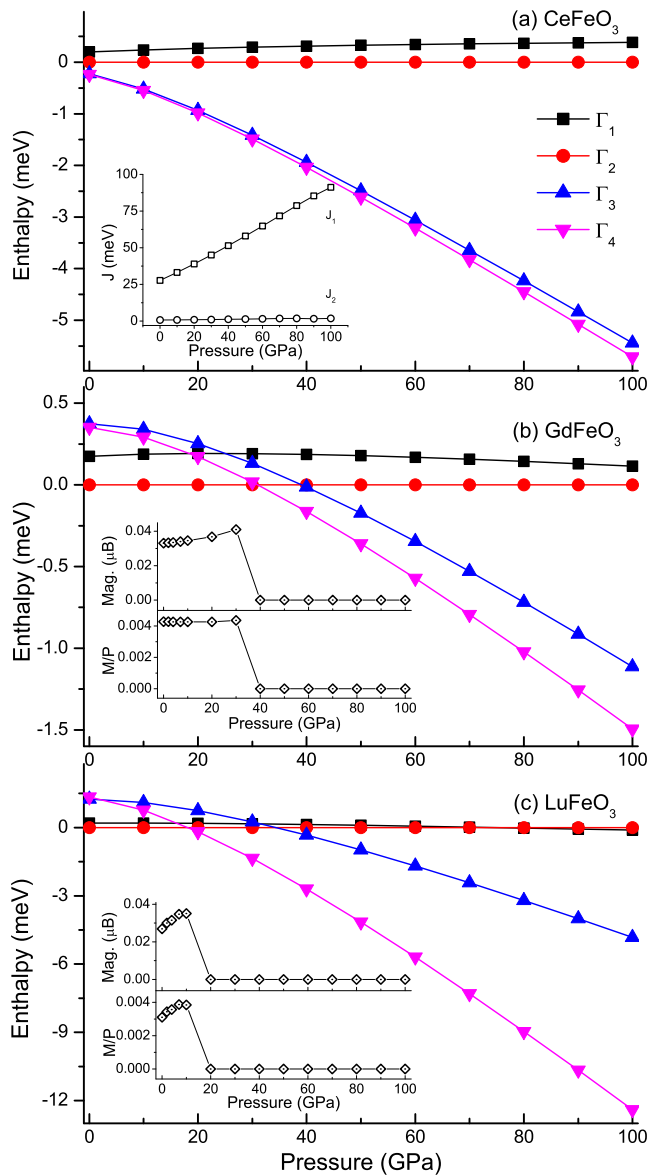


FIG. 4. (Color online) Enthalpies of CeFeO_3 (a), GdFeO_3 (b), and LuFeO_3 (c) as a function of hydrostatic pressure. The enthalpies of Γ_2 are set to zero. The top insets of (b) and (c) show the magnitude of the weak ferromagnetic vector of GdFeO_3 and LuFeO_3 , respectively, versus hydrostatic pressure for the magnetic ground state (which is Γ_2 at low pressure versus Γ_4 at higher pressure). The inset of (a) shows the in-plane and out-of-plane magnetic exchange coefficients between Fe ions. The bottom insets of (b) and (c) show the ratio between the magnetization and polarization (in $\mu_B \text{cm}^2 / \mu\text{C}$ units).

in CeFeO_3 when the pressure varies from 0 to 100 GPa. Such variation naturally implies that the magnetic ordering

temperature is highly adjustable by applying a pressure in these materials.

IV. CONCLUSIONS

In summary, we performed first-principles computations to reveal how structural, electric, magnetic, and magnetoelectric properties of a whole series of hexagonal $R\text{FeO}_3$ rare-earth ferrites (i.e., $R = \text{Ce}, \text{Pr}, \text{Nd}, \text{Pm}, \text{Sm}, \text{Gd}, \text{Tb}, \text{Dy}, \text{Ho}, \text{Er}, \text{Tm}, \text{and Lu}$) depends on chemical and hydrostatic pressures. Several original effects are found. In particular, the electrical polarization is enhanced by a factor of 60% when going from $R = \text{Ce}$ to $R = \text{Lu}$ at atmospheric pressure, and this electrical polarization strengthens as a hydrostatic pressure is applied and increases in magnitude in any hexagonal rare-earth ferrites. These anomalous behaviors of the electrical polarization originate from the improper character of the polarization in this system and the corresponding fact that the primary order parameter is the K_3 phonon mode. Moreover, a magnetic transition, which results in the occurrence (respectively, annihilation) of a weak magnetization is also predicted in hexagonal $R\text{FeO}_3$ compounds with small or intermediate (respectively, large) ionic rare-earth radius. Interestingly, this weak magnetization and resulting linear magnetoelectric effect further suddenly disappear above some critical hydrostatic pressure for small or intermediate rare-earth ionic radius. Hydrostatic pressure therefore allows the possibility of turning on and off linear magnetoelectric effect and weak magnetization.

We are confident that our work deepens the knowledge of room-temperature multiferroics and improper ferroelectrics. We also hope that our first-principles results can be used to construct (complex) phenomenological models, and extract the relevant parameters of these models, aimed at determining and understanding the effect of finite temperature on properties of hexagonal $R\text{FeO}_3$ materials.

ACKNOWLEDGMENTS

We thank Igor Kornev, M. Glazer, and J. Iñiguez for useful discussions. This work is supported by NSF Grant No. DMR-1066158 and ONR Grants No. N00014-11-1-0384 and No. N000-14-12-1-1034. It is also supported by the Ministry of Science and Technology of China (Grant No. 2011CB606405) and National Natural Science Foundation of China (Grant No. 11174173). C.X. thanks the support of State Scholarship Fund from China Scholarship Council. Parts of the calculations were performed on the “Explorer 100” cluster system of Tsinghua. Some computations were also made possible thanks to the MRI Grant No. 0722625, MRI-R2 Grant No. 0959124 and NSF Grant No. 0918970.

- [1] H. Schmid, *Ferroelectrics* **162**, 317 (1994).
- [2] Y. Tokura, *Science* **312**, 1481 (2006).
- [3] N. A. Spaldin, S. W. Cheong, and R. Ramesh, *Phys. Today* **63**(10), 38 (2010).
- [4] J. Wang *et al.*, *Science* **299**, 1719 (2003).

- [5] G. Catalan and J. F. Scott, *Adv. Mater.* **21**, 2463 (2009).
- [6] A. A. Bossak, I. E. Graboy, O. Y. Gorbenko, A. R. Kaul, M. S. Kartavtseva, V. L. Svetchnikov, and H. W. Zandbergen, *Chem. Mater.* **16**, 1751 (2004).

- [7] E. Magome, C. Moriyoshi, Y. Kuroiwa, A. Masuno, and H. Inoue, *Jpn. J. Appl. Phys.* **49**, 09ME06 (2010).
- [8] W. Wang, J. Zhao, J. Shen, X. Xu *et al.*, *Phys. Rev. Lett.* **110**, 237601 (2013).
- [9] H. Das, A. L. Wysocki, Y. Geng, W. Wu, and C. J. Fennie, *Nature Commun.* **5**, 2998 (2014).
- [10] H. Zhao, W. Ren, Y. Yang, X. Chen, and L. Bellaiche, *J. Phys: Condens. Matter* **25**, 466002 (2013).
- [11] G. A. Samara, T. Sakudo, and K. Yoshimitsu, *Phys. Rev. Lett.* **35**, 1767 (1975).
- [12] I. A. Kornev, L. Bellaiche, P. Bouvier, P.-E. Janolin, B. Dkhil, and J. Kreisel, *Phys. Rev. Lett.* **95**, 196804 (2005).
- [13] B. B. VanAken, T. T. M. Palstra, A. Filippetti, and N. A. Spaldin, *Nature Mater.* **3**, 164 (2004).
- [14] C. J. Fennie and K. M. Rabe, *Phys. Rev. B* **72**, 100103 (2005).
- [15] G. Kresse and D. Joubert, *Phys. Rev. B* **59**, 1758 (1999).
- [16] J. P. Perdew, A. Ruzsinszky, G. I. Csonka, O. A. Vydrov, G. E. Scuseria, L. A. Constantin, X. Zhou, and K. Burke, *Phys. Rev. Lett.* **100**, 136406 (2008).
- [17] O. Diéguez, O. E. González-Vázquez, J. C. Wojdel, and J. Íñiguez, *Phys. Rev. B* **83**, 094105 (2011).
- [18] S. J. Yuan, W. Ren, F. Hong, Y. B. Wang, J. C. Zhang, L. Bellaiche, S. X. Cao, and G. Cao, *Phys. Rev. B* **87**, 184405 (2013).
- [19] R. D. King-Smith and D. Vanderbilt, *Phys. Rev. B* **47**, 1651 (1993).
- [20] See <http://www.cryst.ehu.es/cryst/amplimodes.html>.
- [21] A. Muñoz, J. A. Alonso, M. J. Martínez-Lope, M. T. Casáis, J. L. Martínez, and M. T. Fernández-Díaz, *Phys. Rev. B* **62**, 9498 (2000).
- [22] R. D. Shannon, *Acta Crystallogr. A* **32**, 751 (1976).
- [23] Note that we also performed computations with $U = 2$ eV, and that this change of U does not affect the magnetic transition from Γ_2 to Γ_4 when decreasing the rare-earth ionic radius. In other words, $R\text{FeO}_3$ with $R = \text{Ce}$, Pr , and Nd still exhibit a Γ_4 magnetic ground state while the other $R\text{FeO}_3$ compounds possess a Γ_2 magnetic ground state when $U = 2$ eV (exactly as for $U = 4$ eV).
- [24] Note that the hexagonal $P6_3\text{cm}$ phase of the $R\text{FeO}_3$ systems is numerically found to have a higher energy than the orthorhombic $Pnma$ state, even at atmospheric pressure. However, one has also to realize that, despite such hierarchy in energy, this hexagonal phase has been experimentally observed in various $R\text{FeO}_3$ materials. In other words, it is a metastable state. Moreover, we numerically found that the difference in enthalpy between these hexagonal and orthorhombic phases increases with hydrostatic pressure.
- [25] R. E. Cohen and H. Krakauer, *Phys. Rev. B* **42**, 6416 (1990).
- [26] R. E. Cohen, *Nature (London)* **358**, 136 (1992).
- [27] A. Sani, B. Noheda, I. A. Kornev, L. Bellaiche, P. Bouvier, and J. Kreisel, *Phys. Rev. B* **69**, 020105 (2004).
- [28] P. E. Janolin, P. Bouvier, J. Kreisel, P. A. Thomas, I. A. Kornev, L. Bellaiche, W. Crichton, M. Hanfland, and B. Dkhil, *Phys. Rev. Lett.* **101**, 237601 (2008).
- [29] Igor A. Kornev and L. Bellaiche, *Phase Transitions* **80**, 385 (2007).
- [30] The pressure-induced enhancement of the polarization that was predicted in ABO_3 perovskites [12,28,29] was suggested to originate from a pressure-driven hybridization between the $d(e_g)$ orbital of the B transition metal and the $\text{O } 2s$ orbital.
- [31] R. J. Angel, J. Zhao, and N. L. Ross, *Phys. Rev. Lett.* **95**, 025503 (2005).
- [32] H.-Z. Liu, J. Chen, J. Hu, C. D. Martin, D. J. Weidner, D. Häusermann, and H.-K. Mao, *GeoPhys. Res. Lett.* **32**, L04304 (2005).
- [33] H. Zhao, W. Ren, X. Chen, and L. Bellaiche, *J. Phys: Condens. Matter* **25**, 385604 (2013).
- [34] D. Kan, L. Palova, V. Anbusathaiah, C. J. Cheng, S. Fujino, V. Nagarajan, K. M. Rabe, and I. Takeuchi, *Adv. Funct. Mater.* **20**, 1108 (2010).
- [35] We also investigated the effect of U on the critical hydrostatic pressure at which GdFeO_3 undergoes a magnetic transition from Γ_2 to Γ_4 . It is found that such critical pressure increases as U decreases. For instance, it increases from $\simeq 30$ GPa to $\simeq 40$ GPa when U decreases from 4 to 2 eV.
- [36] Note that the amplitudes of the K_3 mode of Fig. 2(c) are first computed in lattice unit, and then multiplied by the lattice constants of the $P6_3/\text{mmc}$ state of hexagonal GdFeO_3 , in order to allow for a relevant comparison between the amplitudes of this mode in different $R\text{FeO}_3$ materials.